

Syntheses and characterization of inorganic–organic hybrids with 4-(isonicotinamido)phthalate and some divalent metal centers

Man-Sheng Chen^{a,b}, Qin Hua^a, Zheng-Shuai Bai^a, Taka-aki Okamura^c, Zhi Su^a, Wei-Yin Sun^{a,*}, Norikazu Ueyama^c

^a Coordination Chemistry Institute, State Key Laboratory of Coordination Chemistry, School of Chemistry and Chemical Engineering, Nanjing National Laboratory of Microstructure, Nanjing University, Nanjing 210093, China

^b Department of Chemistry and Materials Science, Hengyang Normal University, Hengyang 421008, China

^c Department of Macromolecular Science, Graduate School of Science, Osaka University, Toyonaka, Osaka 560-0043, Japan

ARTICLE INFO

Article history:

Received 19 January 2010

Accepted 19 May 2010

Available online 26 May 2010

Keywords:

Inorganic–organic hybrid framework

Magnetic property

Nonlinear optical property

Photoluminescence property

Topology

ABSTRACT

Four new inorganic–organic hybrid frameworks $[\text{Mn}(\text{L})(\text{H}_2\text{O})_2]_n$ (**1**), $\{[\text{Co}(\text{L})(\text{H}_2\text{O})_3] \cdot 2\text{H}_2\text{O} \cdot \text{CH}_3\text{OH}\}_n$ (**2**), $\{[\text{Zn}(\text{L})(\text{H}_2\text{O})] \cdot \text{H}_2\text{O}\}_n$ (**3**) and $[\text{Cd}(\text{HL})_2]_n$ (**4**) [$\text{H}_2\text{L} = 4$ -(isonicotinamido)phthalic acid] have been synthesized and characterized by single-crystal X-ray diffraction analysis. Complex **1** has three-dimensional (3D) structure and topology related to SrAl_2 (sra) with Schläfli symbol of $(4^2 \cdot 6^3 \cdot 8)$. And **2** displays (3,3)-connected two-dimensional (2D) network with $(4,8^2)$ topology, while **3** exhibits a uninodal (3,3)-connected (6,3) 2D network, which is further linked by $\text{N}-\text{H} \cdots \text{O}$ hydrogen bonding interactions to give 3D structure with hms topology and Schläfli symbol of $(6^3)(6^3 \cdot 8)$. Complex **4** with partial deprotonated HL^- ligands also has a 2D network structure. In addition, the magnetic property of **1**, nonlinear optical property of **3** and photoluminescence of **3** and **4** were investigated.

© 2010 Elsevier Ltd. All rights reserved.

1. Introduction

The coordination chemistry of transition metal–carboxylate has attracted great interests of chemists not only because of their fascinating structural diversities, but also due to their interesting properties and potential applications as functional materials in different fields [1–12]. The reported studies showed that the carboxylate groups can adopt varied coordination modes, and as a result metal–carboxylate complexes with diverse structures have been obtained. We focus our attention on study of inorganic–organic hybrids with carboxylate-containing ligands and have obtained various metal complexes with interesting structures and properties in recent years [13–17]. In this context, we have designed a bifunctional carboxylic and pyridine-containing ligand, namely 4-(isonicotinamido)phthalic acid (H_2L), since the multicarboxylate ligands containing N-donors are not well studied, except for the limited examples such as pyridine-2,6-dicarboxylic acid, isonicotinic acid and 5-(isonicotinamido)isophthalic acid [17]. The majority of this research focuses on the synthesis, structural characterization and properties of complexes constructed from different divalent metal salts and H_2L . In this paper, four new hybrids, namely $[\text{Mn}(\text{L})(\text{H}_2\text{O})_2]_n$ (**1**), $\{[\text{Co}(\text{L})(\text{H}_2\text{O})_3] \cdot 2\text{H}_2\text{O} \cdot \text{CH}_3\text{OH}\}_n$ (**2**), $\{[\text{Zn}(\text{L})(\text{H}_2\text{O})] \cdot \text{H}_2\text{O}\}_n$ (**3**) and $[\text{Cd}(\text{HL})_2]_n$ (**4**), were prepared to investigate

the influence of metal ions on the structure of metal–organic frameworks. In addition, the magnetic property of **1**, nonlinear optical property of **3** and photoluminescence of **3** and **4** were investigated (Supplementary data).

2. Experimental

2.1. Materials and measurements

All commercially available solvents and starting materials were used as received without further purification. FT-IR spectra were recorded on a Bruker Vector22 FT-IR spectrophotometer using KBr disks. Elemental analyses for C, H and N were taken on a Perkin–Elmer 240C elemental analyzer at the Analysis Center of Nanjing University. The magnetic susceptibilities in the temperature range of 1.8–300 K were measured on a Quantum Design MPMS7 SQUID magnetometer in a field of 2000 Oe. Diamagnetic corrections were made with Pascal's constants for all samples. The second-order nonlinear optical (NLO) intensity was estimated by measuring a powder sample of 80–150 μm diameter in the form of a pellet relative to urea. A pulsed Q-switched Nd:YAG laser at a wavelength of 1064 nm was used to generate second-harmonic-generation (SHG) signal. The backscattered SHG light was collected by a spherical concave mirror and passed through a filter that transmits only 532 nm radiation. The luminescent spectra for the solid powdered samples were recorded at room

* Corresponding author. Tel.: +86 25 8359 3485; fax: +86 25 8331 4502.
E-mail address: sunwy@nju.edu.cn (W.-Y. Sun).

temperature on an Aminco Bowman Series 2 spectrophotometer with xenon arc lamp as the light source. In the measurements of the emission and excitation spectra, the pass width was 5.0 nm. All the measurements were carried out under the same conditions.

2.2. Synthesis of the ligand 4-(isonicotinamido)phthalic acid (H_2L)

Isonicotinoyl chloride hydrochloride (3.56 g, 20 mmol) was suspended in tetrahydrofuran (40 mL), then triethylamine (4.0 mL) and a solution of 4-aminophthalic acid (3.62 g, 20 mmol) in tetrahydrofuran (40 mL) were added. The mixture was stirred at room temperature for 24 h, the resulting precipitate was filtered, washed with hot water and ethanol, and dried in air to give the ligand (3.6 g, 63%). IR (KBr, cm^{-1}): 3260 (s), 3107 (s), 1717 (m), 1681 (s), 1608 (s), 1532 (s), 1370 (s), 1326 (ms), 849 (m), 772 (s), 656 (ms). 1H NMR (500 MHz, DMSO- d_6): δ 9.06 (s, 2H), 8.74 (s, 1H), 8.32 (s, 1H), 8.20 (s, 1H), 8.04 (s, 1H), 7.94 (s, 2H).

2.3. Synthesis of the complexes

2.3.1. Synthesis of $[Mn(L)(H_2O)_2]_n$ (**1**)

A mixture of H_2L (0.028 g, 0.10 mmol), $MnCl_2 \cdot 4H_2O$ (0.020 g, 0.10 mmol), NaOH (0.008 g, 0.20 mmol), H_2O (8 mL) was kept in a 15 mL Teflon liner autoclave at 140 °C for three days. After the reaction mixture was cooled to room temperature, brown block crystals of complex **1** were collected with a yield of 64%. *Anal. Calc.* for $C_{14}H_{12}MnN_2O_7$ (**1**): C, 44.82; H, 3.22; N, 7.47. Found: C, 44.78; H, 3.29; N, 7.51%. IR (KBr pellet, cm^{-1}): 3421 (s), 1653 (s), 1618 (m), 1580 (s), 1540 (w), 1524 (s), 1407 (m), 1354 (m), 1318 (m), 840 (m), 799 (m), 699 (w), 671 (w), 599 (w).

Table 1
Crystallographic data for **1–4**.

Complex	1	2	3	4
Formula	$C_{14}H_{12}MnN_2O_7$	$C_{15}H_{22}CoN_2O_{11}$	$C_{14}H_{12}ZnN_2O_7$	$C_{28}H_{18}CdN_4O_{10}$
Formula weight	375.20	465.20	385.63	682.86
Crystal system	monoclinic	monoclinic	orthorhombic	monoclinic
Space group	$P2_1/n$	$C2/c$	$Pca2_1$	$P2_1/n$
a (Å)	6.4311(7)	21.764(3)	24.636(8)	9.1382(10)
b (Å)	30.353(3)	7.3700(11)	7.932(3)	11.8973(13)
c (Å)	7.2962(8)	24.119(4)	7.200(2)	22.921(3)
α (°)	90.00	90.00	90.00	90.00
β (°)	92.134(2)	95.197(3)	90.00	92.059(2)
γ (°)	90.00	90.00	90.00	90.00
V (Å ³)	1423.3(3)	3852.8(10)	1407.1(9)	2490.4(5)
Z	4	8	4	4
T (K)	293(2)	293(2)	200	293(2)
μ (mm^{-1})	0.971	0.952	1.790	0.950
D_{calc} (g/m^3)	1.751	1.570	1.820	1.821
$F(000)$	764	1848	784	1368
Reflections collected	7384	9299	12773	12390
Unique reflections	4488	2639	3396	3174
Goodness-of-fit (GOF) on F^2	0.940	1.070	1.037	0.992
R_{int}	0.0776	0.0971	0.0584	0.0500
$R_1 [I > 2\sigma(I)]$	0.0394	0.0596	0.0403	0.0398
$wR_2 [I > 2\sigma(I)]$	0.1037 ^a	0.1503 ^b	0.0935 ^c	0.0651 ^d
Residuals (e Å ⁻³)	-0.565, 0.586	-0.529, 0.838	-0.667, 0.461	-0.427, 0.819

$$^a w = 1/[\sigma^2(F_0)^2 + (0.1685P)^2 + 0.1685P], \text{ where } P = (F_0^2 + 2F_c^2)/3.$$

$$^b w = 1/[\sigma^2(F_0)^2 + (0.0728P)^2], \text{ where } P = (F_0^2 + 2F_c^2)/3.$$

$$^c w = 1/[\sigma^2(F_0)^2 + (0.0490P)^2 + 1.4963P], \text{ where } P = (F_0^2 + 2F_c^2)/3.$$

$$^d w = 1/[\sigma^2(F_0)^2 + (0.0150P)^2], \text{ where } P = (F_0^2 + 2F_c^2)/3.$$

2.3.2. Synthesis of $\{[Co(L)(H_2O)_3] \cdot 2H_2O \cdot CH_3OH\}_n$ (**2**)

A mixture of H_2L (0.028 g, 0.10 mmol), $Co(NO_3)_2 \cdot 6H_2O$ (0.030 g, 0.10 mmol), NaOH (0.008 g, 0.20 mmol), CH_3OH (2 mL) and H_2O (6 mL) was sealed in a 15 mL Teflon liner autoclave at 140 °C for three days. After cooling to room temperature, pink platelet crystals of complex **2** were collected with a yield of 44%. *Anal. Calc.* for $C_{15}H_{22}CoN_2O_{11}$ (**2**): C, 38.72; H, 4.77; N, 6.02. Found: C, 38.64; H, 4.81; N, 5.97%. IR (KBr pellet, cm^{-1}): 3425 (s), 1672 (s), 1618 (s), 1586 (s), 1534 (m), 1404 (m), 1384 (s), 797 (m), 709 (m), 665 (w), 621 (w).

2.3.3. Synthesis of $\{[Zn(L)(H_2O)] \cdot H_2O\}_n$ (**3**)

The preparation of **3** is similar to that of **1** except that $MnCl_2 \cdot 4H_2O$ was replaced by $Zn(NO_3)_2 \cdot 6H_2O$ (0.029 g, 0.10 mmol). After cooling to room temperature, colorless platelet crystals of **3** were collected in 52% yield. *Anal. Calc.* for $C_{14}H_{12}ZnN_2O_7$ (**3**): C, 43.60; H, 3.14; N 7.26. Found: C, 43.63; H, 3.20; N, 7.21%. IR (KBr

Table 2
Selected bond lengths (Å) and angles (°) for **1–4**.

1^a			
Mn(1)–O(1)	2.192(2)	Mn(1)–O(2)#1	2.178(2)
Mn(1)–O(1W)	2.109(2)	Mn(1)–O(3)#2	2.171(1)
Mn(1)–O(2W)	2.156(2)	Mn(1)–N(2)#3	2.324(2)
O(1)–Mn(1)–O(1W)	91.80(7)	O(1W)–Mn(1)–N(2)#3	87.54(6)
O(1)–Mn(1)–O(2W)	90.77(6)	O(2)#1–Mn(1)–O(2W)	88.91(6)
O(1)–Mn(1)–O(3)#2	84.47(6)	O(2W)–Mn(1)–O(3)#2	88.80(6)
O(1)–Mn(1)–N(2)#3	91.22(6)	O(2W)–Mn(1)–N(2)#3	85.96(6)
O(1W)–Mn(1)–O(2)#1	89.14(6)	O(2)#1–Mn(1)–O(3)#2	90.16(6)
O(1W)–Mn(1)–O(3)#2	97.88(6)	O(2)#1–Mn(1)–N(2)#3	94.11(6)
2^b			
Co(1)–O(1)	2.176(3)	Co(1)–O(3W)	2.103(3)
Co(1)–O(1W)	2.087(3)	Co(1)–N(1)#1	2.132(4)
Co(1)–O(2W)	2.099(3)	Co(1)–O(3)#2	2.080(3)
O(1)–Co(1)–O(1W)	90.2(1)	O(1W)–Co(1)–O(3)#2	84.3(1)
O(1)–Co(1)–O(2W)	169.3(1)	O(2W)–Co(1)–O(3W)	88.6(1)
O(1)–Co(1)–O(3W)	85.6(1)	O(2W)–Co(1)–N(1)#1	86.8(1)
O(1)–Co(1)–N(1)#1	84.8(1)	O(2W)–Co(1)–O(3)#2	89.0(1)
O(1)–Co(1)–O(3)#2	99.9(1)	O(3W)–Co(1)–N(1)#1	95.2(1)
O(1W)–Co(1)–O(2W)	96.6(1)	O(3)#2–Co(1)–O(3W)	89.6(1)
O(1W)–Co(1)–N(1)#1	91.3(1)		
3^c			
Zn(1)–O(2)	1.970(3)	Zn(1)–N(11)	2.034(3)
Zn(1)–O(31)#1	1.945(3)	Zn(1)–O(41)#2	1.924(3)
O(2)–Zn(1)–N(11)	112.6(1)	O(2)–Zn(1)–O(31)#1	100.9(1)
O(2)–Zn(1)–O(41)#2	112.8(2)	O(31)#1–Zn(1)–N(11)	109.1(1)
O(41)#2–Zn(1)–N(11)	99.1(1)	O(31)#1–Zn(1)–O(41)#2	122.7(2)
4^d			
Cd(1)–O(1)	2.304(3)	Cd(1)–O(2)	2.579(3)
Cd(1)–N(4)	2.277(3)	Cd(1)–N(2)#1	2.358(3)
Cd(1)–O(2)#2	2.398(3)	Cd(1)–O(6)#3	2.513(3)
Cd(1)–O(7)#3	2.306(2)		
O(1)–Cd(1)–O(2)	52.92(9)	O(2)–Cd(1)–N(2)#1	94.79(9)
O(7)#3–Cd(1)–N(2)#1	81.74(9)	O(2)–Cd(1)–O(2)#2	78.70(9)
O(1)–Cd(1)–N(4)	102.7(1)	O(2)–Cd(1)–O(6)#3	137.50(8)
O(2)#2–Cd(1)–O(6)#3	141.34(8)	O(2)–Cd(1)–O(7)#3	167.2(1)
O(2)#2–Cd(1)–O(7)#3	88.65(9)	N(2)#1–Cd(1)–N(4)	167.2(1)
O(1)–Cd(1)–N(2)#1	90.0(1)	O(2)#2–Cd(1)–N(4)	86.9(1)
O(1)–Cd(1)–O(2)#2	130.57(9)	O(6)#3–Cd(1)–N(4)	101.6(1)
O(6)#3–Cd(1)–O(7)#3	54.30(8)	O(7)#3–Cd(1)–N(4)	89.23(9)
O(1)–Cd(1)–O(6)#3	84.72(9)	O(2)#2–Cd(1)–N(2)#1	83.9(1)
O(1)–Cd(1)–O(7)#3	139.0(1)	O(6)#3–Cd(1)–N(2)#1	80.4(1)
O(2)–Cd(1)–N(4)	92.06(9)		

^a Symmetry transformations used to generate equivalent atoms: #1: $1 + x, y, z, -z + 1/2$, #2: $1 - x, 1 - y, -z$, #3: $1/2 + x, 1/2 - y, -1/2 + z$.

^b Symmetry transformations used to generate equivalent atoms: #1: $x + 1/2, -y + 3/2, z + 1/2$, #2: $-x + 3/2, y + 1/2, -z + 3/2$.

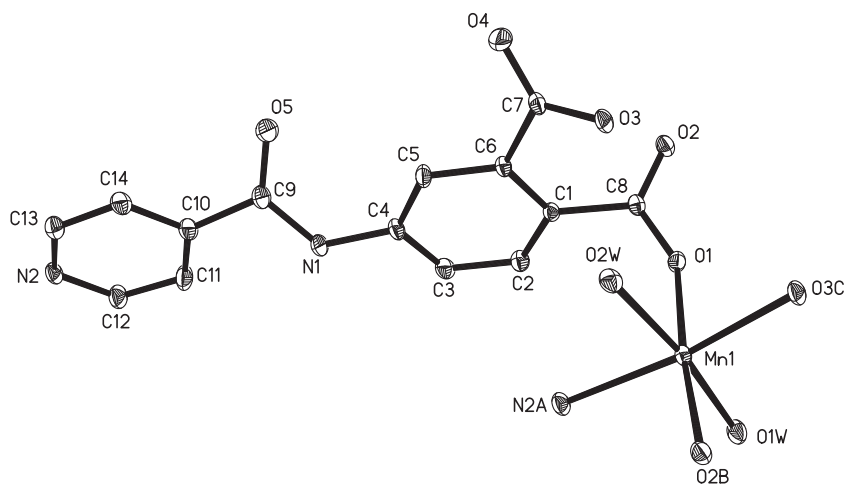
^c Symmetry transformations used to generate equivalent atoms: #1: $1 - x, 1 - y, -1/2 + z$, #2: $-1/2 + x, 1 - y, z$.

^d Symmetry transformations used to generate equivalent atoms: #1: $1/2 - x, -1/2 + y, 5/2 - z$, #2: $1 - x, 1 - y, 2 - z$, #3: $-1/2 + x, 1/2 - y, 1/2 + z$.

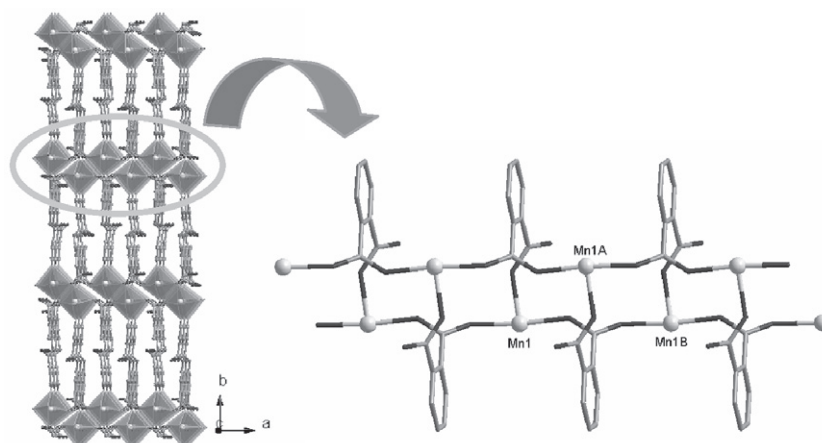
pellet, cm^{-1}): 3424 (s), 1678 (s), 1611 (m), 1556 (m), 1528 (m), 1499 (w), 1425 (m), 1384 (s), 1324 (m), 1068 (m), 790 (m), 694 (w), 674 (w), 585 (w).

2.3.4. Synthesis of $[\text{Cd}(\text{HL})_2]_n$ (**4**)

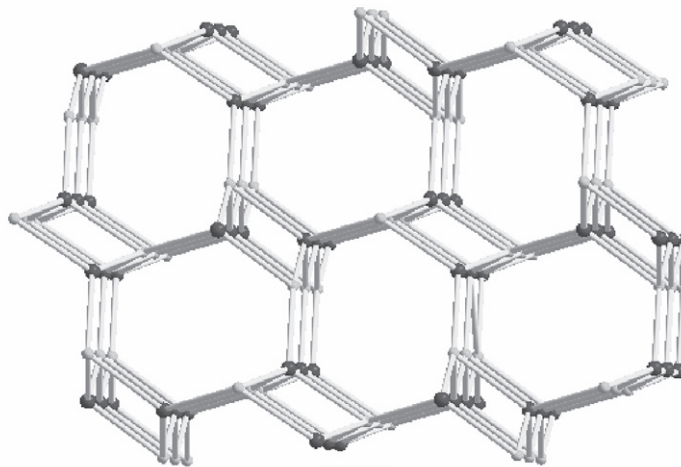
The title complex was prepared by layering method. An aqueous solution (5 mL) of H_2L (0.028 g, 0.10 mmol) was carefully ad-



(a)



(b)



(c)

Fig. 1. (a) Coordination environment of Mn(II) atom in **1** with the ellipsoids drawn at the 30% probability level, hydrogen atoms were omitted for clarity. (b) 3D framework of the polymer that possesses a 1D rectangular channel along *c*-axis. (c) The extended framework topology of **1** is congruent with that of **sra**.

justed to pH 6 by using tetrabutylammonium hydroxide (10%) solution and placed at the bottom of a test tube. Then a buffer layer of a solution (5 mL) of methanol/H₂O (1:1) was layered over it, and afterward, a solution of Cd(NO₃)₂·4H₂O (0.031 g, 0.10 mmol) in methanol (5 mL) was layered over the buffer layer. Colorless block crystals of **4** were collected in 38% yield after 20 days. *Anal. Calc.* for C₂₈H₁₈CdN₄O₁₀ (**4**): C, 49.25; H, 2.66%; N, 8.20. Found: C, 49.21; H, 2.70; N, 8.17%. IR (KBr pellet, cm⁻¹): 3425 (s), 1699 (s), 1673 (s), 1616 (vs), 1584 (vs), 1535 (m), 1404 (m), 1382 (s), 797 (m), 710 (m), 667 (w), 624 (w).

2.4. Crystal structure determination

Crystallographic data of **1**, **2** and **4** were collected at 293 K on a Bruker SMART CCD system equipped with graphite-monochromated Mo K α radiation ($\lambda = 0.71073$ Å) using $\omega - \varphi$ scan technique. The data integration and empirical absorption corrections were carried out by SAINT programs [18]. The structures were solved by direct methods (SHELXS 97) [19]. All the non-hydrogen atoms were refined anisotropically on F^2 by full-matrix least-squares techniques (SHELXL 97) [20]. All the hydrogen atoms except for those of water molecules were generated geometrically and refined isotropically using the riding model, while those of water molecules in **1** were found directly. Crystallographic data collection for complex **3** was carried out on a Rigaku RAXIS-RAPID Imaging Plate diffractometer at 200 K, using graphite-monochromated Mo K α radiation ($\lambda = 0.71075$ Å). The structure of **3** was solved by direct methods with SIR92 [21] and expanded using Fourier techniques [22]. All the non-hydrogen atoms were refined anisotropically on F^2 by full-matrix least-squares methods. All the hydrogen atoms of ligands in **3** were generated geometrically. Details of the crystal parameters, data collection and refinements for **1–4** are summarized in Table 1. Selected bond lengths and angles for **1–4** are listed in Table 2.

3. Results and discussion

3.1. Crystal structures of complexes **1–4**

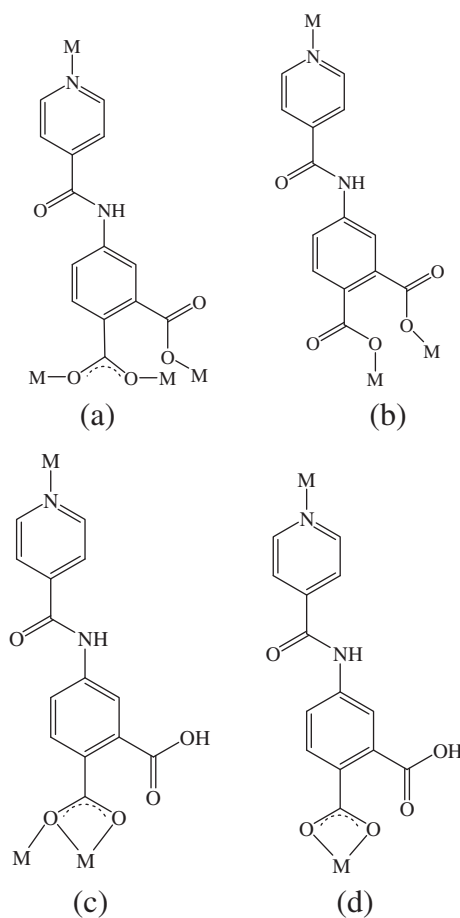
3.1.1. [Mn(L)(H₂O)₂]_n (**1**)

The result of X-ray crystallographic analysis revealed that complex **1** crystallizes in monoclinic space group $P2_1/n$ (Table 1). As shown in Fig. 1a, each Mn(II) atom is six-coordinated with distorted octahedral coordination geometry by one pyridyl nitrogen (N2A) and three carboxylate oxygen (O1, O2B, O3C) atoms from four different L²⁻ ligands, and two oxygen (O1W, O2W) atoms from two terminal coordinated water molecules. The Mn1–O bond distances in **1** range from 2.1086(16) to 2.1924(16) Å, and the Mn1–N one is 2.324(2) Å, and the coordination angles around Mn(II) vary from 84.47(6) to 174.62(6)° as listed in Table 2. It is noteworthy that the two carboxylate groups of each L²⁻ ligand connect three Mn(II) atoms with different coordination modes of $\mu_1-\eta^1:\eta^0$ monodentate and $\mu_2-\eta^1:\eta^1$ bis-monodentate, respectively, in addition the pyridyl group of each L²⁻ coordinates with one Mn(II) (Scheme 1a). Therefore, the coordination interactions between the four-connecting L²⁻ ligand and six-coordinated Mn(II) atom as described above make **1** a three-dimensional (3D) framework. Firstly, one-dimensional (1D) [Mn(OCO)]_∞ double chain is formed by the connections between the carboxylate groups of L²⁻ and Mn(II) atoms if the coordination of pyridyl group with Mn(II) is neglected (Fig. 1b). The inter- and intra-chain Mn–Mn distances of Mn1–Mn1A and Mn1–Mn1B (Fig. 1b) are 5.20 Å and 6.43 Å, respectively. Then, the 1D chains are cross-linked by pyridyl groups of L²⁻, leading to the formation of 3D extended framework of **1** with 1D rectangular channels (Fig. 1b).

In order to better identify the nature of the structure of complex **1**, suitable connectors can be defined by using the topological approach [23–25]. As discussed above, each L²⁻ ligand is neighbored by four Mn(II) atoms, and thus can be considered as a four-connector. Meanwhile, the central Mn(II) atom can also be viewed as a four-connector by omitting the coordination of two terminal water molecules. Analysis of the vertex symbols and coordination sequence of **1** revealed that its topology is related to SrAl₂ (**sra**) with Schläfli symbol of (4²·6³·8) as depicted in Fig. 1c. Namely a net has been referred by Smith as the ABW tetrahedral net in Li-ABW zeolite while O’Keeffe and Hyde refer it as the **sra** net [26–29].

3.1.2. {[Co(L)(H₂O)₃]}·2H₂O·CH₃OH]_n (**2**)

When the H₂L ligand was used to react with Co(NO₃)₂·6H₂O, NaOH at 140 °C for three days, complex **2** was isolated. The structure of **2** was studied by X-ray single-crystal structure determination. The asymmetric unit of **2** consists of one Co(II) atom, one L²⁻ ligand, three coordinated and two free water molecules, and one uncoordinated methanol molecule. The coordination environment of Co(II) atom in **2** is shown in Fig. 2a with atom numbering scheme. Each Co(II) atom is coordinated by one pyridyl nitrogen (N1B) and two carboxylate oxygen (O1, O3A) atoms from three distinct L²⁻ ligands and three oxygen atoms (O1W, O2W, O3W) from three water molecules, respectively. The bond angles around the Co(II) atom are in the range of 84.33(12)–173.55(13)° (Table 2), and thus the coordination geometry of the Co(II) atom is distorted octahedral with NO₅ donor set. The Co1–N bond length is 2.132(4) Å and the Co1–O ones are in the range from 2.080(3) to 2.176(3) Å (Table 2). On the other hand, each L²⁻ ligand in **2** uses



Scheme 1. Coordination modes of H₂L ligand in complexes **1–4**.

its pyridyl and two carboxylate groups to connect three Co(II) atoms. Different from those in complex **1**, the two carboxylate groups of each L^{2-} ligand in **2** have the same coordination mode of $\mu_1-\eta^1:\eta^0$ -monodentate (Scheme 1b).

In complex **2**, the Co(II) atoms are linked together by the carboxylate groups of L^{2-} to form an infinite 1D zigzag chain if the Co–N connections are neglected, which is further linked together through the Co–N coordination leading to the formation of a two-dimensional (2D) network (Fig. 2b). As described above, each Co(II) is surrounded by three L^{2-} ligands and each L^{2-} ligand links three Co(II) atoms. Thus, both Co(II) atom and L^{2-} ligand can be considered as three-connected nodes in a ratio of 1:1 in **2**. Therefore, the complex **2** exhibits a (3,3)-connected 2D network with $(4,8^2)$ topology as clearly shown in Fig. 2c. Furthermore, as depicted in Fig. 2d, the 2D layers packed together through N–H...O, O–H...O and C–H...O hydrogen bonding interactions to give a 3D framework. The hydrogen bonding data are summarized in Table S1.

3.1.3. $\{[Zn(L)(H_2O)]\cdot H_2O\}_n$ (**3**)

When $Zn(NO_3)_2\cdot 6H_2O$, instead of $MnCl_2\cdot 4H_2O$ used in preparation of **1**, was used to react with ligand H_2L , complex **3** with a 2D layer structure was obtained. The results of X-ray crystallographic analysis indicate that the Zn(II) atom in **3** has distorted tetrahedral coordination geometry with two oxygen (O31A, O41B) atoms and one nitrogen (N11) atom from three separated L^{2-} ligands and

one aqua ligand (O2) (Fig. 3a), with Zn–O bond distances ranging from 1.924 (3) to 1.970(3) Å and Zn1–N bond length of 2.034(3) Å (Table 2). Each L^{2-} ligand acts as a three-connector to link three Zn(II) atoms in complex **3** (Scheme 1b), which is similar to that in **2**, namely each carboxylate group displays $\mu_1-\eta^1:\eta^0$ -monodentate mode and two carboxylate groups connect two Zn(II) atoms, the pyridyl nitrogen atom binds to another Zn(II) atom, consequently resulting in formation of a 2D layer structure (Fig. 3b).

Similar topological method was used to get insight of the structure of **3**. As discussed above, both each Zn(II) and L^{2-} ligand can be defined as three-connecting nodes since they connect three L^{2-} ligands and three metal ions, respectively, then a 2D network with (6,3) topology is yielded as illustrated in Fig. 3c, which is different from those in complexes **1** and **2**. Furthermore, the most striking feature of **3** is that the 2D (6,3) networks are connected together through the N–H...O together with C–H...O hydrogen-bonding interactions (Table S1) to produce a 3D framework (Fig. S1) with **hms** topology and Schläfli symbol of $(6^3)(6^9\cdot 8)$ by taking the N1–H1...O32 hydrogen-bonding interaction into account (Fig. 3d) [30]. The different structures of complexes **1–3** showed that the metal ions play crucial role in determining the structure of the frameworks.

3.1.4. $[Cd(HL)_2]_n$ (**4**)

When the reaction of ligand H_2L with $Cd(NO_3)_2\cdot 4H_2O$ was carried out by layering method, rather than the hydrothermal reaction

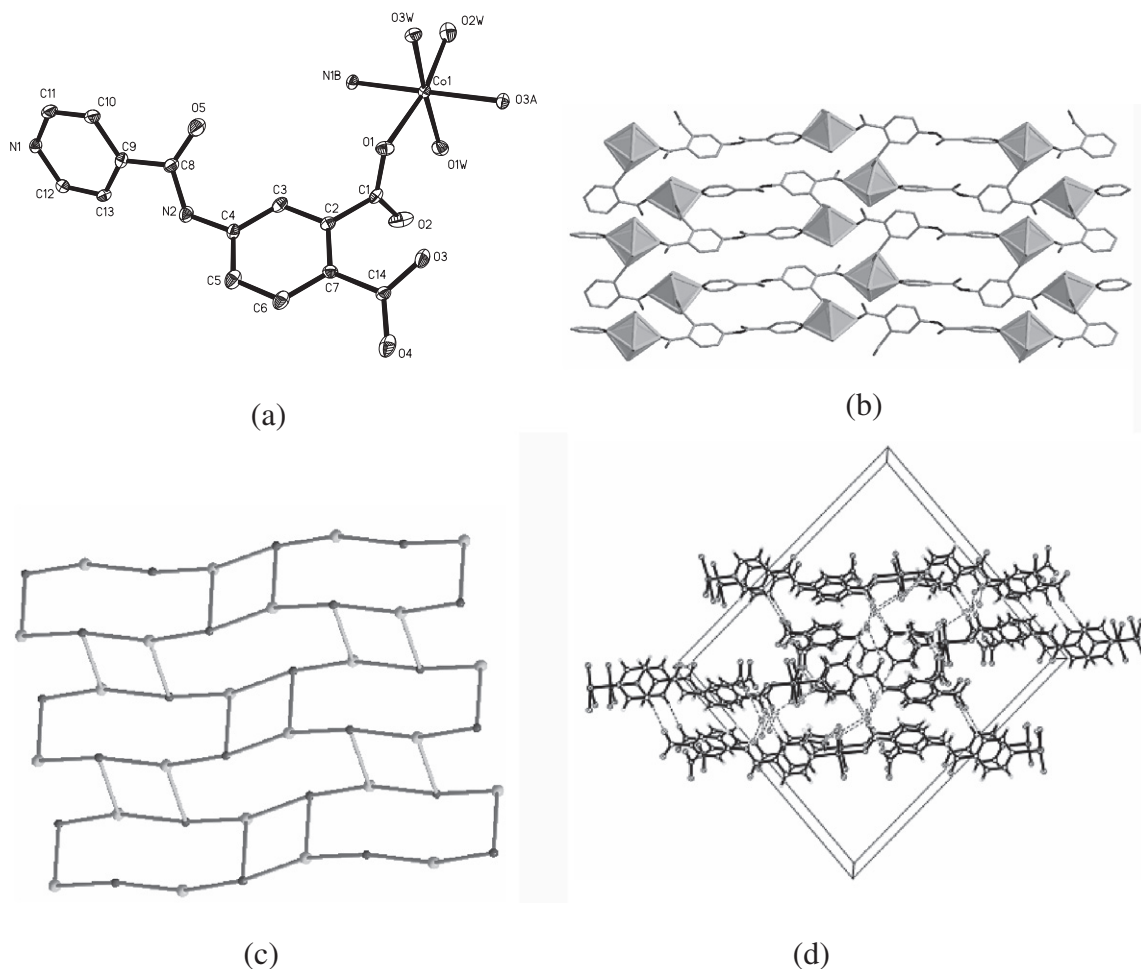


Fig. 2. (a) Coordination environment of Co(II) in **2** with the ellipsoids drawn at the 30% probability level, hydrogen atoms and guest molecules were omitted for clarity. (b) Polyhedral representation of the 2D layer structure in **2**. (c) A uninodal 3-connected 2D $(4,8^2)$ network of complex **2**. (d) 3D packing structure of **2** with hydrogen bonds indicated by the dashed lines.

used for preparation of **1–3**, a new compound **4** was obtained. The crystallographic data showed that complex **4** crystallizes in monoclinic $P2_1/n$ space group and the Cd(II) atom has a pentagonal bipyramid coordination geometry with a N_2O_5 donor set (Fig. 4a). It should be noticed that in contrast to the complete deprotonation of H_2L to give L^{2-} in **1–3**, the H_2L is only partial deprotonated to generate HL^- in **4** as confirmed by crystallographic and IR spectral data (a strong IR band from $-COOH$ appeared at 1699 cm^{-1} , see Section 2). As shown in Scheme 1c and d, the carboxylate groups of two different HL^- ligands in **4** have different coordination modes of $\mu_2-\eta^1:\eta^2$ bridging to link two Cd(II) and $\mu_1-\eta^1:\eta^1$ chelating to connect one Cd(II). Such coordination interactions between the

two- and three-connecting HL^- ligands and seven-coordinated Cd(II) atom as described above make **4** a 2D network with Cd_2O_2 rhombic subunit as depicted in Fig. 4b. The 2D networks are further connected together by $N-H\cdots O$ and $C-H\cdots O$ hydrogen bonds to give a 3D framework (Fig. S2, Table S1).

3.2. Properties

3.2.1. Magnetic property

As described above, the Mn(II) atoms are bridged by $\mu_2-\eta^1:\eta^1$ bis-monodentate carboxylate groups to give $[Mn(OCO)]_\infty$ chain in **1** (Fig. 1b), and magnetic interactions may exist between the

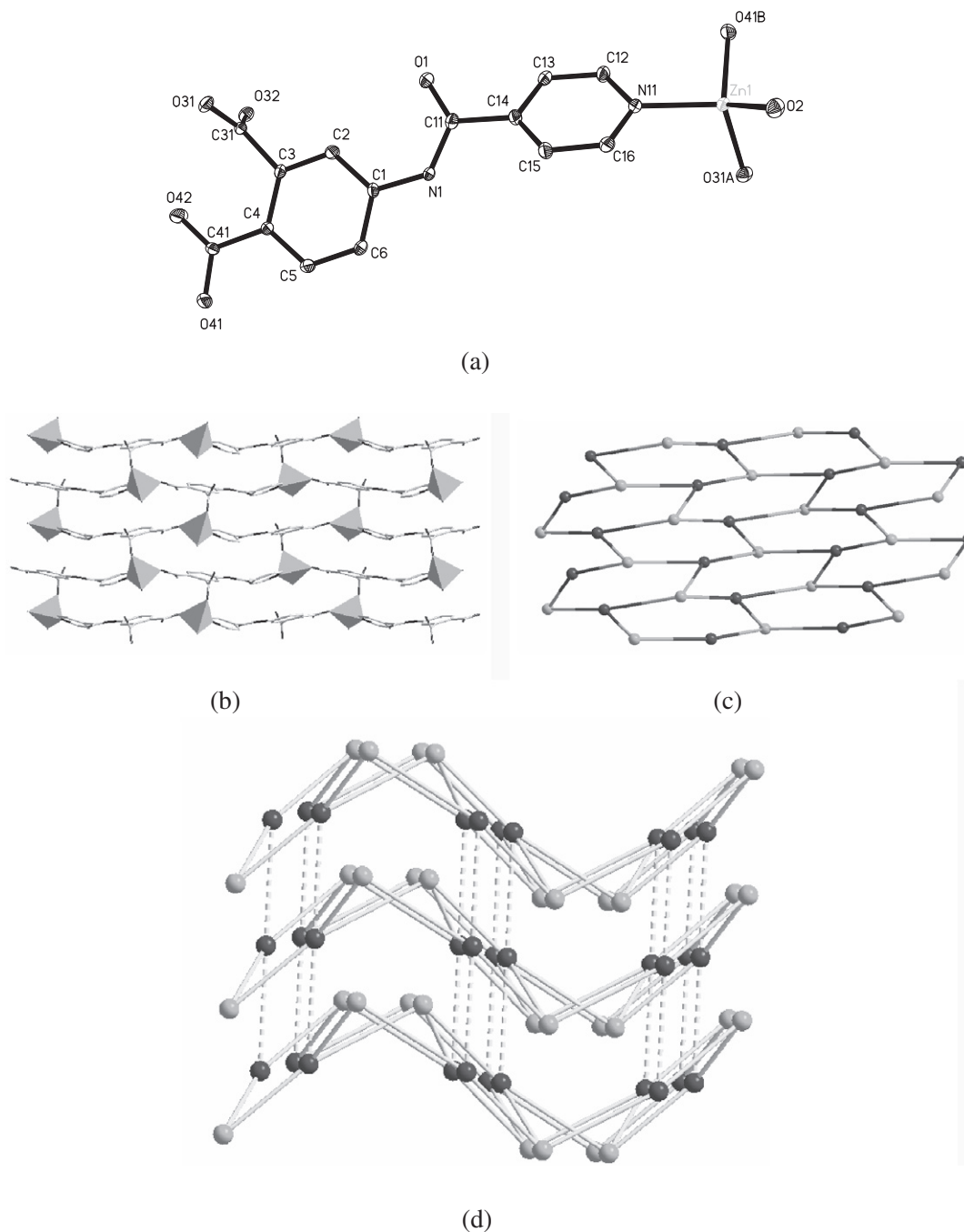


Fig. 3. (a) Coordination environment of Zn(II) in **3** with the ellipsoids drawn at the 30% probability level, hydrogen atoms and water molecules were omitted for clarity. (b) Polyhedral representation of the 2D layer structure in **3**. (c) A uninodal 3-connected 2D (6,3) network of complex **3**. (d) 3D hms net of **3** linked by hydrogen bonding shown by dashed line.

Mn(II) atoms. Therefore, the temperature dependence of magnetic susceptibilities of **1** was measured in the range of 300–1.8 K with an applied magnetic field of 2000 Oe. As depicted in Fig. S3, the $\chi_M T$ value is 4.23 emu K mol⁻¹ at room temperature, which is close to the value of 4.37 emu K mol⁻¹ expected for one magnetically independent Mn(II) ($S = 5/2$) center. The $\chi_M T$ decreases steadily with decreasing temperature and reaches a value of 0.62 emu K mol⁻¹ at 1.8 K, indicating an overall antiferromagnetic behavior between the Mn(II) ions. According to the structural data, such magnetic behavior indicates the antiferromagnetic coupling within the [Mn(OCO)]_∞ chain unit in **1** while the inter-chain interactions and the coupling through the pyridyl groups of L²⁻ are negligible. Therefore, the magnetic interaction can be fitted to the isotropic Hamiltonian $H = -2J\sum S_i S_{i+1}$, and the analytical expression derived by Fisher for the 1D Heisenberg chain of classical spins ($S = 5/2$) was used [31–35]. The results revealed that the best least-square fit of the theoretical equation to experimental data gave $g = 2.03$, $J = -0.54$ cm⁻¹, $TIP = 0.0008$ cm⁻¹ and the agreement factor $R = \sum [(\chi_M T)_{\text{obsd}} - (\chi_M T)_{\text{calcd}}]^2 / \sum (\chi_M T)_{\text{obsd}}^2$ is 1.0×10^{-5} . The negative J value further confirms the existence of antiferromagnetic interactions in **1**.

3.2.2. Nonlinear optical property of **3**

It is known that a non-centrosymmetric structure may have second-order non-linear optical (NLO) effects, and due to the

advantages over pure organic or inorganic compounds, new NLO made up by organic-inorganic hybrid coordination polymers are especially interested [36,37]. Complex **3** crystallizes in acentric space group $Pca2_1$, thus quasi-Kurtz second-harmonic-generation (SHG) measurements were performed on powder sample of **3** to confirm its acentricity as well as to evaluate its potential application as second-order NLO material [38]. The preliminary result showed the bulk materials of **3** display modest powder SHG activity with a response of approximately 0.5 times of that for urea.

3.2.3. Luminescent properties

In general, fluorescence properties of inorganic-organic hybrid coordination complexes, especially with d^{10} metal centers, have been investigated owing to their potential applications as photoactive materials [39–41]. In this study, the photoluminescence properties of **3** and **4** as well as Na₂L were investigated in the solid state at room temperature and the results are shown in Fig. S4. Intense emissions were observed at 452 nm ($\lambda_{\text{ex}} = 360$ nm) for Na₂L, 465 nm ($\lambda_{\text{ex}} = 360$ nm) for **3**, 466 nm ($\lambda_{\text{ex}} = 360$ nm) for **4**, respectively. Such emissions can be attributed to neither metal-to-ligand charge transfer (MLCT) nor ligand-to-metal charge transfer (LMCT) because the Zn(II)/Cd(II) ions are in d^{10} configuration and difficult to oxidize or to reduce. Therefore the emissions observed in **3** and **4** are tentatively considered to be attributed to the $\pi-\pi^*$ intraligand photoluminescence due to their resemblance to that of

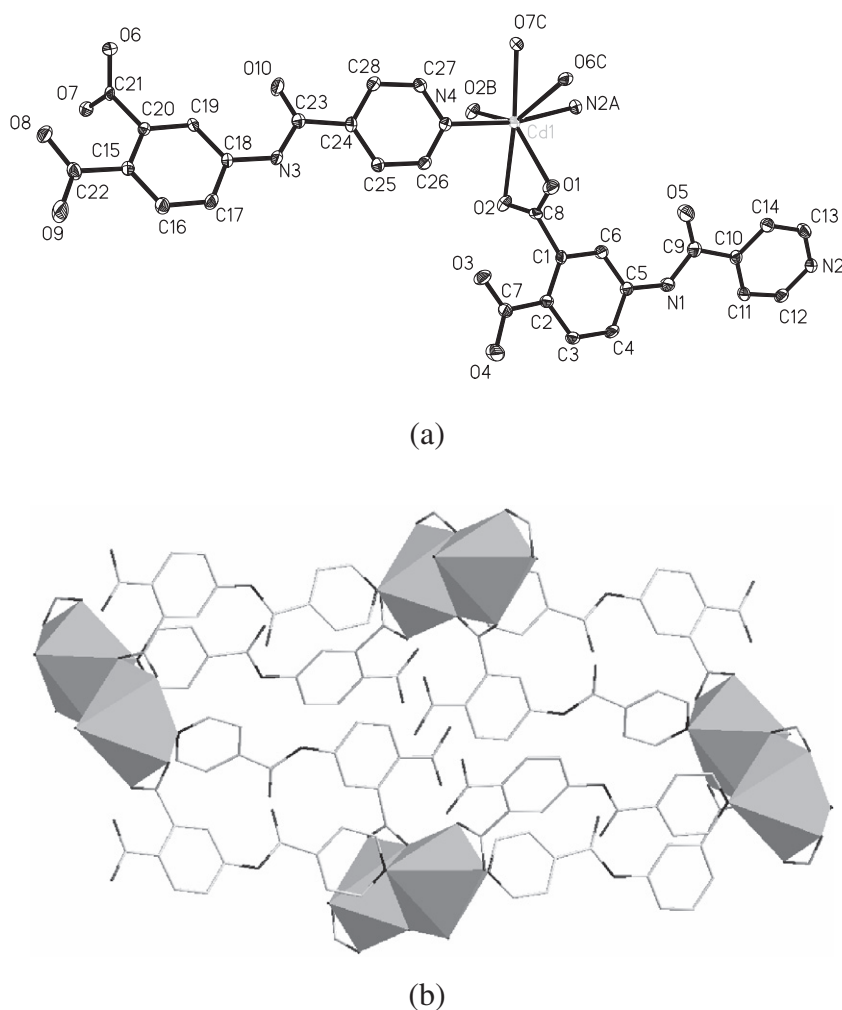


Fig. 4. (a) Coordination environment of Cd(II) in **4** with the ellipsoids drawn at the 30% probability level, hydrogen atoms were omitted for clarity. (b) Polyhedral representation of the 2D layer structure in **4**.

Na₂L ligand, and the slight red-shifts of **3** and **4** compared to that of Na₂L probably result from the fact that the coordination of L to Zn(II)/Cd(II) increases the ligand conformational rigidity and thus reduces the non-radiative energy loss [42–44].

4. Conclusions

In summary, we have successfully synthesized four new hybrids based on a new pyridine- and carboxylate-containing ligand **4**- (isonicotinamido)phthalic acid with corresponding metal salts. The results revealed that it is promising to build up specific structures via combining transition metals and pyridyl-carboxylate ligands. The varied coordination modes of the ligand found in the present work prove that it is a useful building block in the preparation of novel hybrid frameworks with potential magnetic and luminescent properties.

Acknowledgments

This work was financially supported by the National Natural Science Foundation of China (Grant Nos. 20731004 and 20721002) and the National Basic Research Program of China (Grant Nos. 2007CB925103 and 2010CB923303).

Appendix A. Supplementary data

CCDC 760534, 760535, 760536, and 7605347 contain the supplementary crystallographic data for **1**, **2**, **3** and **4**. These data can be obtained free of charge via <http://www.ccdc.cam.ac.uk/conts/retrieving.html>, or from the Cambridge Crystallographic Data Centre, 12 Union Road, Cambridge CB2 1EZ, UK; fax: (+44) 1223 336 033; or e-mail: deposit@ccdc.cam.ac.uk. Supplementary data associated with this article can be found, in the online version, at doi:10.1016/j.poly.2010.05.014.

References

- [1] J. Mroziński, *Coord. Chem. Rev.* 249 (2005) 2534.
- [2] J.L. Atwood, *Nat. Mater.* 1 (2002) 91.
- [3] M. Eddaoudi, J. Kim, N. Rosi, D. Vodak, J. Wachter, M. O'Keeffe, O.M. Yaghi, *Science* 295 (2002) 469.
- [4] R.Q. Zou, H. Sakurai, S. Han, R.Q. Zhong, Q. Xu, *J. Am. Chem. Soc.* 129 (2007) 8402.
- [5] X.J. Kong, Y.P. Ren, L.S. Long, Z.P. Zheng, R.B. Huang, L.S. Zheng, *J. Am. Chem. Soc.* 129 (2007) 7016.
- [6] N. Guillou, C. Livage, W. van Beek, M. Noguès, G. Férey, *Angew. Chem., Int. Ed.* 42 (2003) 643.
- [7] S. Ghosh, P.S. Mukherjee, *Dalton Trans.* (2007) 2542.
- [8] M. Dan, C.N.R. Rao, *Angew. Chem., Int. Ed.* 45 (2006) 281.
- [9] A.Y. Robin, K.M. Fromm, *Coord. Chem. Rev.* 250 (2006) 2127.
- [10] L. Pan, H.M. Liu, X.G. Lei, X.Y. Huang, D.H. Olson, N.J. Turro, J. Li, *Angew. Chem., Int. Ed.* 42 (2003) 542.
- [11] X.L. Wang, C. Qin, E.B. Wang, Y.G. Li, C.W. Hu, L. Xu, *Chem. Commun.* (2004) 378.
- [12] S. Kitagawa, R. Kitaura, S.-i. Noro, *Angew. Chem., Int. Ed.* 43 (2004) 2334.
- [13] J. Xu, Z.S. Bai, T.-a. Okamura, M.S. Chen, W.Y. Sun, N. Ueyama, *Polyhedron* 28 (2009) 2480.
- [14] Q. Chu, G.X. Liu, T.-a. Okamura, Y.Q. Huang, W.Y. Sun, N. Ueyama, *Polyhedron* 27 (2008) 812.
- [15] Z.S. Bai, Z.P. Qi, Y. Lu, Q. Yuan, W.Y. Sun, *Cryst. Growth Des.* 8 (2008) 1924.
- [16] Z.S. Bai, J. Xu, T.-a. Okamura, M.S. Chen, W.Y. Sun, N. Ueyama, *Dalton Trans.* (2009) 2528.
- [17] M.S. Chen, Z.S. Bai, Z. Su, S.S. Chen, W.Y. Sun, *Inorg. Chem. Commun.* 12 (2009) 530.
- [18] SAINT, Program for Data Extraction and Reduction, Bruker AXS, Inc., Madison, WI, 2001.
- [19] G.M. Sheldrick, SHELXS-97, Program for the Solution of Crystal Structures, University of Göttingen, Germany, 1997.
- [20] G.M. Sheldrick, SHELXL-97, Program for Refinement of Crystal Structures, University of Göttingen, Germany, 1997.
- [21] SIR92: A. Altomare, M.C. Burla, M. Camalli, M. Casciaro, C. Giacovazzo, A. Guagliardi, G. Polidori, *J. Appl. Crystallogr.* 27 (1994) 435.
- [22] DIRFID 94: P.T. Beurskens, G. Admiraal, G. Beurskens, W.P. Bosman, R. de Gelder, R. Israel, J.M.M. Smits, The DIRFID-94 Program System; Technical Report of the Crystallography Laboratory, University of Nijmegen, Nijmegen, The Netherlands, 1994.
- [23] N.W. Ockwig, O. Delgado-Friederichs, M. O'Keeffe, O.M. Yaghi, *Acc. Chem. Res.* 38 (2005) 176.
- [24] O.M. Yaghi, H. Li, C. Davis, D. Richardson, T.L. Groy, *Acc. Chem. Res.* 31 (1998) 474.
- [25] S.R. Batten, R. Robson, *Angew. Chem., Int. Ed.* 37 (1998) 1460.
- [26] K.E. Holmes, P.F. Kelly, M.R.J. Elsegood, *Dalton Trans.* (2004) 3488.
- [27] P.S. Wang, C.N. Moorefield, M. Panzer, G.R. Newkome, *Chem. Commun.* (2005) 465.
- [28] M. O'Keeffe, M. Eddaoudi, H.L. Li, T. Reineke, O.M. Yaghi, *J. Solid State Chem.* 152 (2000) 3.
- [29] N.L. Rosi, M. Eddaoudi, J. Kim, M. O'Keeffe, O.M. Yaghi, *Angew. Chem., Int. Ed.* 41 (2002) 284.
- [30] O.V. Dolomanov, A.J. Blake, N.R. Champness, M. Schröder, *J. Appl. Crystallogr.* 36 (2003) 1283.
- [31] M.E. Fisher, *Am. J. Phys. (Paris)* 32 (1964) 343.
- [32] C.J. O'Connor, *Prog. Inorg. Chem.* 29 (1982) 203.
- [33] R.H. Wang, D.Q. Yuan, F.L. Jiang, L. Han, S. Gao, M.C. Hong, *Eur. J. Inorg. Chem.* (2006) 1649.
- [34] J. Li, S.B. Tang, L. Lu, H.C. Zeng, *J. Am. Chem. Soc.* 129 (2007) 9401.
- [35] W. Chen, Q. Yue, C. Chen, H.M. Yuan, W. Xu, J.S. Chen, S.N. Wang, *Dalton Trans.* (2003) 28.
- [36] H.S. Ra, K.M. Ok, P.S. Halasyamani, *J. Am. Chem. Soc.* 125 (2003) 7764.
- [37] J.S.O. Evans, S. Bénard, P. Yu, R. Clément, *Chem. Mater.* 13 (2001) 3813.
- [38] L. Song, S.W. Du, J.D. Lin, H. Zhou, T. Li, *Cryst. Growth Des.* 7 (2007) 2268.
- [39] A. Vogler, H. Kunkely, *Coord. Chem. Rev.* 250 (2006) 1622.
- [40] R.Q. Fan, D.S. Zhu, Y. Mu, G.H. Li, Y.L. Yang, Q. Su, S.H. Feng, *Eur. J. Inorg. Chem.* (2004) 4891.
- [41] L.L. Wen, Y.Z. Li, Z.D. Lu, J.G. Lin, C.Y. Duan, Q.J. Meng, *Cryst. Growth Des.* 6 (2006) 530.
- [42] U.H.F. Bunz, *Chem. Rev.* 100 (2000) 1605.
- [43] W.Y. Yang, H. Schmider, Q.G. Wu, Y.S. Zhang, S.N. Wang, *Inorg. Chem.* 39 (2000) 2397.
- [44] Y.B. Chen, J. Zhang, J.K. Cheng, Y. Kang, Z.J. Li, Y.G. Yao, *Inorg. Chem. Commun.* 7 (2004) 1139.